A Systematic Study of Elementary Reactions in the NH_3 deNO_x Process

J. PARK and M. C. LIN
Department of Chemistry, Emory University, Atlanta, GA 30322, USA
e-mail: jpark05@emory.edu and chemmcl@emory.edu

Abstract — The kinetics and mechanisms of the $NH_2 + NO_x$ (x =1, 2) reactions have been systematically studied using a pulsed laser photolysis/mass spectrometric technique. The total rate constants and product branching ratios for the two reactions have been tested by measuring the time-resolved concentrations of H_2O, N_2O and NO_2 in the laser-initiated reaction of NH_3 with NO in the presence of varying amounts of NO_2 in the temperature range of 300 - 725 K. The measured concentrations can be quantitatively accounted for by our comprehensive mechanism, confirming our reported product branching ratio for $NH_2 + NO_2 \rightarrow N_2O + H_2O$, $\beta_{2b} = 0.19 \pm 0.02$ over the temperature range investigated. Futhermore, our comprehensive mechanism also accounts reasonably for the concentration profiles of NH_3, NO_2 and N_2O reported by Glarborg and coworkers (1995) in their study of the isothermal reaction of NH_3 with NO_2.

Key words: NH_3 deNO_x process, $NH_2 + NO_x$

INTRODUCTION

Recently, there has been substantial interest in the efficiency of NH_3 as a deNO_x agent (Lyon, 1976). The interest stems, in part, from the controversy and uncertainty in the product branching probabilities of the two pivotal elementary reactions involved in the deNO_x process: $NH_2 + NO_x$ (x=1, 2) which generates radical and molecular products (see, e.g., Silver and Kolb, 1982; Atakan et al., 1989; Bulatov *et al.*, 1989; Stephens, *et al.*, 1993; Brown and Smith, 1994; Vandooren, *et al.*, 1994; Glarborg *et al.*, 1995; Park and Lin, 1996a; 1996b; 1997a; 1997b):

$$NH_2 + NO \rightarrow NNH + OH \quad (1a)$$
$$\rightarrow N_2 + H_2O \quad (1b)$$

$$NH_2 + NO_2 \rightarrow H_2NO + NO \quad (2a)$$
$$\rightarrow N_2O + H_2O \quad (2b)$$

OH and H, which can be generated by the decomposition of NNH and H_2NO formed in reactions (1a) and (2a), respectively, are the key chain carriers in the system. Their production enhances the chain process by reacting with NH_3. Because the competitive branching reactions (1b) and (2b) are effectively chain termination steps, the magnitudes of the rate constants for (1a) and (2a) or their branching ratios strongly influence the efficacy of NH_3 as an NO_x reducing agent.

In order to reliably measure the branching ratios of the pivotal reactions (1a) and (2a), we have carried out a series of experiments employing a pulsed-laser photolysis/mass spectrometry (PLP/MS) technique covering a broad range of temperatures, 300-1200 K (Park and Lin, 1996a; 1996b; 1997a; 1997b). We determined the total rate constants for the reactions and their product branching ratios which yielded the following expressions:

T = 300-1000 K

$$k_{1a} = 8.4 \times 10^9\ T^{0.53}\ e^{+502/T}$$
$$k_{1b} = 8.3 \times 10^{14}\ T^{-0.93}\ e^{+192/T}$$
$$k_{2a} = 6.5 \times 10^{16}\ T^{-1.44}\ e^{-135/T}$$
$$k_{2b} = 1.6 \times 10^{16}\ T^{-1.44}\ e^{-135/T}$$

T = 1000-2000 K

$$k_{1a} = 9.2 \times 10^{22}\ T^{-3.02}\ e^{-4826/T}$$
$$k_{1b} = 3.4 \times 10^{14}\ T^{-0.98}\ e^{+1311/T}$$

where the absolute rate constants are given in units of $cm^3/(mole.s)$.

The above kinetic data for product branching in reaction (1), NH_2 + NO, resulted from our determination that the branching ratio for OH production from (1a), α_{1a}, increases gradually from 0.10 at 300 K to 0.28 at 1000 K, with a sharp increase to 0.48 at 1200 K (Park and Lin, 1996a; 1997a). The drastic upturn of α_{1a} above 1000 K confirms the result of our recent study of the NH_3 + NO reaction by Fourier transform infrared (FTIR) spectrometry (Halbgewachs *et al.*, 1996) and the conclusion reached by the modeling of NH_3 - NO flame speeds that $\alpha_{1a} = 0.5$ above 1500 K (Vandooren *et al.*, 1994; Brown and Smith, 1994).

The product branching for reaction (2) was measured over the temperature range of 300 - 990 K (Park and Lin, 1996b; 1997b). The total rate constant and the branching ratio for N_2O production, $\beta_{2b} = k_{2b}/(k_{2a} + k_{2b})$, were determined concurrently by time-resolved mass spectrometry and the rate constants given above resulted from this study. β_{2b} was found to be independent of temperature, 0.19 ± 0.02, in the range investigated. This result agrees with that reported by Quandt and Hershberger (1996), 0.14 ± 0.03, at room temperature and with that reached by kinetic modeling of the $NH_3 + NO_2$ reaction in the temperature range of 850-1350 K by Glarborg *et al.* (1995). However, our result is inconsistent with the large value of $\beta_{2b} = 0.59 \pm 0.03$ at room temperature reported by Meunier *et al.* (1996).

In this study, we performed a new set of kinetic measurements designed to test the validity of the rate constants given above and to resolve the discrepancy regarding the value of β_{2b}. Absolute yields of H_2O and N_2O as well as the decay of NO_2 concentration in the laser-induced reaction of mixtures containing varying amounts of NH_3, NO and NO_2 were measured in 300 - 725 K. The results of kinetic modeling of the data substantiate the value of the total rate constant, $k_2 = k_{2a} + k_{2b}$, and the branching ratio for N_2O production, $k_{2b}/k_2 = 0.19 \pm 0.02$ in the temperature regime studied.

These and other results obtained by kinetic modeling of the NH_3 + NO_x reactions are reported herein.

EXPERIMENTAL

The total rate constant and product branching ratio determination were carried out with the LPL/MS system schematically depicted in Fig. 1. The combination of the high-pressure mass-spectrometric sampling technique of Saalfeld and coworkers (Wyatt *et al.*, 1974, 1975) with the pulse laser photolysis method for free radical generation and reactions has been described in the work of Gutman

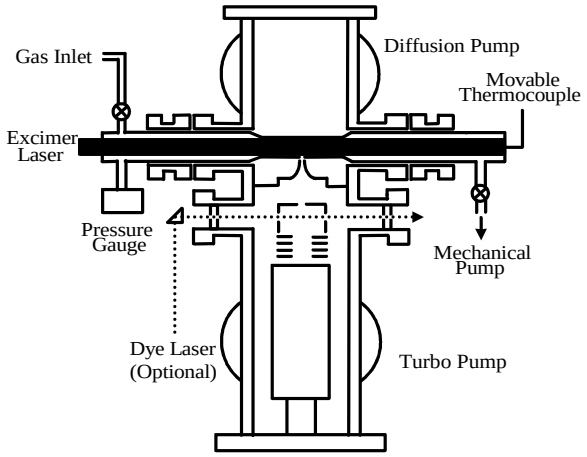

Figure 1. Schematic diagram of the experimental appratus.

and coworkers (Russel *et al.*, 1988) and our recent series of publications (Park and Lin, 1996a,b; 1997a,b).

The reactor is a quartz tube of about 10 mm i.d. and 150 mm length. It can be heated from room temperature to 1200 K with a uniformity and reliability of 2 K. The reactor has a 120 μm diameter conical sampling hole aligned with the sampling axis of the quadrupole mass spectrometer (Extrel model C50 QMS). The highest achievable pressure in the reactor with He as carrier gas is 10 torr, which resulted in the pressure rise in the expansion chamber (pumped by a 1300 l/s Edwards Diffstak model 160/700 diffusion pump) from 10^{-7} to 10^{-4} torr and in the QMS chamber (pumped by a 1000 l/s Leybold turbomolecular pump) from 10^{-8} to 10^{-5} torr.

The NH_2 radical was generated by the photolysis of NH_3 at 193 nm (Lambda Physik EMG 102). The initial concentration of NH_2 radicals can be determined accurately from the amount of NH_3 fragmented in the absence of NO_x. The addition of NO_x enhanced the conversion of NH_3 and the formation of H_2O (m/z = 18) and N_2O (m/z = 44). These masses were initially present at small noise levels; the signal-to-noise ratios for these and other masses were typically S/N = 10-20 which gave rise to excellent time- and mass-resolved signals with a Nicolet 450 Digital Waveform Acquisition System employed in conjunction with a microcomputer. Figure 2 shows the typical measured and kinetically modeled H_2O and N_2O product profiles and NO (in the absence of NO_2) and NO_2 reactant profiles. The addition of NO_2 produces N_2O from reaction (2b) with a concomitant enhanced yield of H_2O, whose presence made the quantitative determination of NH_3 (m/z = 17) impossible because of its overlapping with OH^+ (m/z = 17).

All experiments were carried out under slow flow conditions. The mixing of reactants (NH_3, NO_2 and NO) and the He carrier gas was achieved in a 25-cm stainless bellows tube prior to their introduction into the reactor. The flow rates of individual gases were measured with mass flowmeters (Brooks, model 5850 C and MKS, model 0258 C).

NH_3 (Aldrich), CO (Matheson Gas Products), CO_2 (Aldrich) and H_2O (deionized water) were purified by standard trap-to-trap distillation using appropriate coolants. NO (Matheson) was purified by vacuum distillation using a dehydrated silica gel trap maintained at 195 K to remove NO_2 impurity. The silica gel trap was preheated overnight for debydration with continuous diffusion-pumping. NO_2 (Aldrich) was purified by trap-to-trap distillation at dry ice temperature. The NO_2 sample was pre-treated with several torr of pure O_2 and mixed overnight for the conversion of NO impurity to NO_2. He (99.9995%, Specialty Gases) was used without further purification.

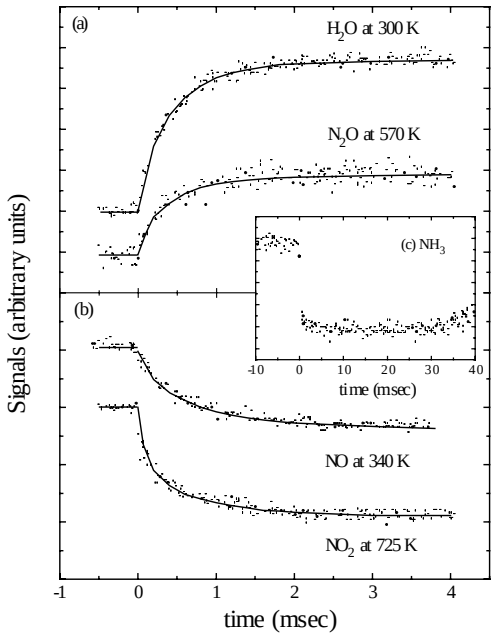

Figure 2. Typical time-resolved transient signals in the NH_3/NO_x system. The experimental conditions were varied. Solid lines represent the kinetically modeled results.

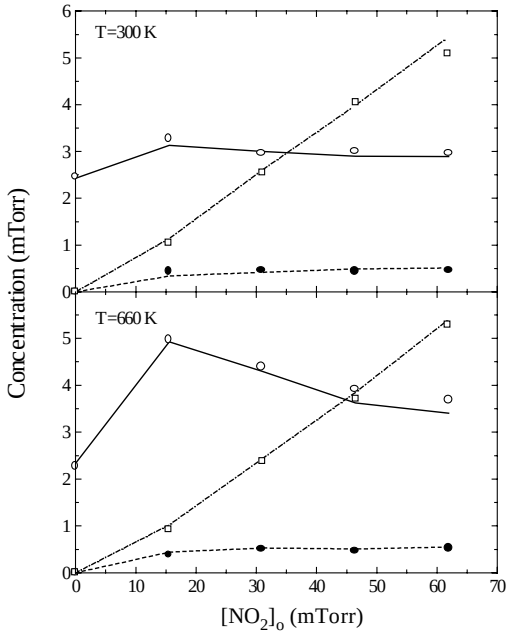

Figure 3. The product and reactant concentrations as functions of initial NO_2 pressure in the $NH_3/NO/NO_2$ system. ○, H_2O; □, NO_2; ●, N_2O. Lines represent the kinetically modeled results.

RESULTS AND DISCUSSION

The time-resolved signals of H_2O, N_2O, NO (in the absence of NO_2), and NO_2 shown in Fig. 2 can be directly converted into concentration profiles using the results of calibration with standard mixtures sampled under exactly the same pressures as employed in the experimental runs. Figure 3 shows typical sets of data obtained at 300 and 660 K. The experimental conditions used for these and the other two temperatures studied are summarized in Table I.

Temp	Initial conditions					Experiment			Modeling		
(K)	$[NH_3]_o$	$[NH_2]_o$	$[NO]_o$	$[NO_2]_o$	$[O]_o$	$[H_2O]_t$	$[N_2O]_t$	$[NO_2]_t$	$[H_2O]_t$	$[N_2O]_t$	$[NO_2]_t$
300	25.4	2.38	12.8	0.00	0.00	2.46	0.00	0.00	2.43	0.00	0.00
	25.4	2.38	13.0	15.4	0.12	3.27	0.43	10.5	3.13	0.34	11.4
	25.4	2.38	13.1	30.7	0.24	2.97	0.46	25.3	3.00	0.42	26.0
	25.4	2.38	13.3	46.0	0.35	3.00	0.44	40.3	2.90	0.49	39.9
	25.4	2.38	13.4	61.3	0.47	2.97	0.46	50.6	2.89	0.51	54.5
449	26.1	1.64	12.8	0.00	0.00	1.62	0.00	0.00	1.76	0.00	0.00
	26.1	1.64	13.0	15.3	0.21	2.96	0.40	11.3	2.91	0.33	11.5
	26.1	1.64	13.2	30.6	0.42	2.68	0.43	25.7	2.45	0.38	26.3
	26.1	1.64	13.4	45.9	0.63	2.60	0.35	40.8	2.33	0.40	44.4
	26.1	1.64	13.6	61.2	0.83	2.27	0.36	50.5	2.24	0.40	55.5
660	44.5	2.10	21.5	0.00	0.00	2.26	0.00	0.00	2.33	0.00	0.00
	44.5	2.10	21.8	15.2	0.34	4.98	0.38	9.24	4.93	0.44	10.2
	44.5	2.10	22.2	30.3	0.67	4.39	0.51	23.9	4.30	0.53	24.3
	44.5	2.10	22.5	45.5	1.01	3.92	0.46	37.0	3.62	0.51	38.5
	44.5	2.10	22.8	60.7	1.35	3.68	0.52	52.8	3.40	0.55	54.0
725	41.0	2.39	20.0	0.00	0.00	2.63	0.00	0.00	2.50	0.00	0.00
	41.0	2.39	20.4	14.1	0.35	5.18	0.42	8.36	5.05	0.45	8.05
	41.0	2.39	20.7	28.2	0.70	4.29	0.55	21.9	4.20	0.53	22.2
	41.0	2.39	21.0	42.3	1.05	4.47	0.51	35.5	4.20	0.55	35.5

TABLE I. Reaction Conditions and Product Yields at Temperatures Studied. The units of all concentrations are in mTorr.

The absolute concentrations of H_2O, N_2O and NO_2 can be unambiguously measured with no mass-overlapping problem which would invalidate the reliable determination of NH_3 in the presence of NO_x. For NO, the presence of NO_2 also renders its quantitative concentration determination unreliable on account of the extensive fragmentation of NO_2^+ to NO^+.

In Fig. 2, we compared the measured concentration profiles of H_2O, N_2O, NO (in the absence of NO_2) and NO_2 with the predicted profiles as fuctions of time using the mechanism and rate constants summarized in Appendix. Kinetic modeling was carried out with the SENKIN program (Kee *et al.*, 1989 and Lutz *et al.*, 1988). The agreement between the predicted and measured time-resolved concentrations is excellent. In Fig. 3, the measured concentrations of H_2O, N_2O and NO_2 at 10 ms after laser initiation as functions of the initial concentration of NO_2 are compared with the predicted values at 300 and 660 K. An equally good agreement is achieved. The concentrations measured at 10 ms after laser initiation correspond to the limiting plateau values which involve, in principle, all possible primary, secondary and tertiary reactions. The results of sensitivity analyses indicate, however, the chemistry of the NH_2-NO_x system is dominated primarily by reactions (1) and (2), and the reaction of H and OH with NH_3, NO_2, HNO and HONO.

In order to test the reliability of our reported product branching ratio for N_2O production from $NH_2 + NO_2$ via (2b), in Fig. 4 we compared the results of kinetic modeling at 300 K using $\beta_{2b} = 0.19$ (Park and Lin, 1996b) and $\beta_{2b} = 0.59$ (Meunier *et al.*, 1996), represented by solid and dashed curves, respectively. The use of the higher value of β_{2b} by Meunier *et al.* leads to the over-production of N_2O and H_2O. Also, the consumption of the NO_2 reactant is apparently slower with the larger value of β_{2b}. Essentially the same result was obtained by using both β_{2b} and the smaller value of k_2 reported by Meunier *et al.*

Kinetic Modeling of the $NH_3 + NO_2$ Reactions

Glarborg and coworkers (1994, 1995) studied the NH_3/NO_x system using an isothermal flow reactor and provided a detailed reaction mechanism for the system. Their experimental and kinetically modeled values are shown in Fig. 5 in comparison with our modeled results. As shown in the figure, our modeled results except NO are in close agreement with their experimental values, while their modeled values of NH_3 and NO_2 are evidently higher than the experimental values. In their mechanism, they employed the branching ratio of the reaction (1a) at 1200 K is ~ 0.30 which is somewhat lower than our 0.45 ± 0.05 and the branching ratio of the reaction (2a) at 1200 K is ~ 0.15 which is relatively close to our 0.19 ± 0.02. Our higher branching ratio for reaction (1a) produces the more highly reactive chain reaction carriers, OH and H, which is easily generated by the

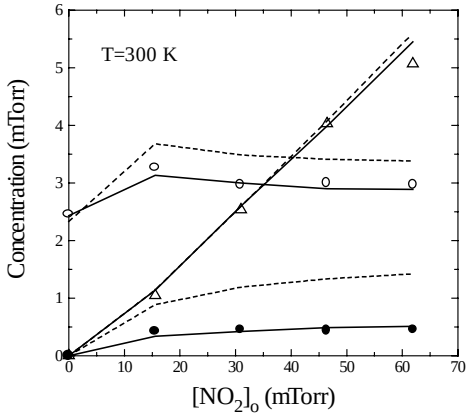

Figure 4. The product and reactant concentrations as functions of initial NO_2 pressure in the $NH_3/NO/NO_2$ system. ○, H_2O; □, NO_2 (÷10); ●, N_2O. Solid line, kinetic modeling results with $k_2 = 1.49\times10^{13}$ cm^3/mole·sec and $\beta_{2b} = 0.19$ (Park and Lin, 1997b); dashed line, kinetic modeling results with the same value of k_2 and $\beta_{2b} = 0.59$ (Meunier *et al.*, 1996).

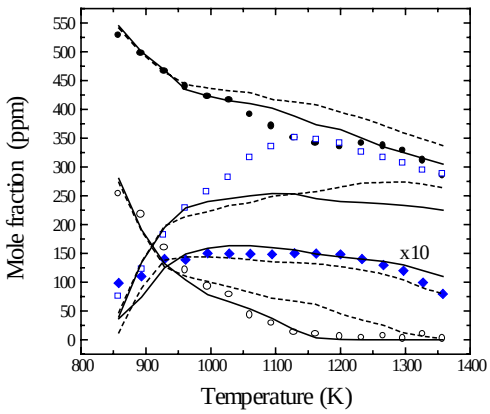

Figure 5. Comparison of experimental data (Glarborg *et al*., 1994) and kinetic modeling results for the NH_3/NO_2 system. ●, NH_3; □, NO; ○, NO_2; ◆, N_2O (×10). Dotted line, Garlborg's modeling result; solid line, our modeling result. Initial conditions: NH_3 = 547 ppm, NO_2 = 285 pm, NO = 35 ppm. Residence time = 110/T s (T in Kelvin) and P = 1.05 atm.

dissociation of the weakly bound NNH radical. The reactions of NH_3 with OH and H radicals generate more NH_2 radicals and thus enhance the efficiency of NO_x reduction.

However, the NO discrepancy is quite perplexing. In order to account for this discrepancy, we examined the N atom mass balance by taking into account stable N-species, NH_3, NO, NO_2, N_2O and N_2. Since N_2 was not measured in Glarborg's experiments, we used the predicted value instead. Other nitrogen containing molecules were negligible according to the results of kinetic modeling. The result indicates that the total N-contents above 1000 K, $[NH_3]_e + [NO]_e + [NO_2]_e + 2\,[N_2O]_e + 2\,[N_2]_m$, is always greater than the initial nitrogen content, $[NH_3]_o + [NO]_o + [NO_2]_o$, by as much as 100 ppm; where $[X]_e$, $[X]_m$ and $[X]_o$ represent the experimental, kinetically modeled, and initial concentrations, respectively. The apparent gain in nitrogen-atom contents resulted from the observed high yield of NO which cannot be accounted for by both theoretical models.

CONCLUSION

In this study we have demonstrated that the major products formed in the laser-initiated reaction of NH_3 with NO_x between 300 amd 725 K, N_2O and H_2O can be quantitatively modeled kinetically. In addition the consumption of NO_2, can be satisfactorily accounted for by the mechanism used.

The same mechnism was also employed to model the thermal reaction of NH_3 with NO_2 between 800 and 1350 K measured by Glarborg *et al*.; the concentrations of all species reported NH_3, NO_2 and N_2O (except NO above 1000 K) could be reasonably modeled. The origin of the perflexing deviation between the observed and predicted NO concentrations requires further investigation.

Acknowledgment. The authors gratefully acknowledge the support of this work from the Office of Naval Research (contract No. N00014-89-J-1949) under the direction of Dr. R. S. Miller.

REFERENCES

Atakan, B., Jacobs, A., Wahl, M. and Wolfrum, J (1989). Kinetic Measurements and Product Branching Ratio for the Reaction NH_2 + NO at 294-1027 K. *Chem. Phys. Lett*., **155**, 609-613.

Diau, E. W. G., Yu, T., Wagner, M. A. G. and Lin, M. C. (1994). Kinetics of the NH_2 + NO Reaction: Effects of Temperature on the Total Rate Constant and the OH/H_2O Branching Ratio. *J. Phys. Chem*., **98**, 4034 -4042.

Glarborg, P., Dam-Johansen, K. and Miller, J. A. (1995) The Reaction of Ammonia with Nitrogen Dioxide in a Flow Reactior: Implications for the NH_2 + NO_2 Reaction. *Int. J. Chem. Kinet*., **27**, 1207-1210.

Glarborg, P., Dam-Johansen, K., Miller, J. A., Kee, R. J. and Coltrin, M. E. (1994). Modeling the Thermal DENOx Process in Flow Reactors. Surface Effects and Nitrous Oxide Formation. *Int. J. Chem. Kinet*., **26**, 421-436.

Halbgewachs, M. J., Diau, E. W. G., Mebel, A. M., Lin, M. C. and Melius, C. F. (1996). Thermal Reduction of NO by NH_3: Kinetic Modeling of the NH_2 + NO Product Branching Ratio. *26th Symp. (Int.) Combust*., 2109-2115.

Lyon, R. K. (1976). The NH_3-NO-O_2 Reaction. *Int. J. Chem. Kinet*. **8**, 315-318.

Kee, R. J., Rupley, F. M. and Miller, J. A. CHEMKIN-II: A Fortran Chemical Kinetics Package for the Analysis of Gas-Phase Chemical Kinetics; Sandia National Laboratories Report No. SAND 89-8009, 1989.

Lutz, A.E., Kee, R.J. and Miller, J.A. SENKIN: A Fortran Program for Predicting Homogeneous Gas-Phase Chemical Kinetics with Sensitivity Analysis, Sandia National Laboratories, Report No. SAND87-8248, 1988.

Meunier, H., Pagsberg, P. and Sillesen, A. (1996) Kinetics and Branchiong Ratios for the Reactions $NH_2 + NO_2 \rightarrow N_2O + H_2O$ and $NH_2 + NO_2 \rightarrow H_2NO + NO$ Studied by Pulse Radiolysis Combined with Time-resolved Infrared Diode Lase Spectroscopy, *Chem. Phys. Lett*., **261**, 277-282.

Park, J. and Lin, M. C. (1996a). Direct Determination of Product Branching for the NH_2 + NO Reaction at Temperatures between 302 and 1,060 K. *J. Phys. Chem*., **100**, 3317-19.

Park, J. and Lin, M. C. (1996b). Mass-Spectrometric Determination of Product Branching Probabilities in the NH_2 + NO_2 Reaction at Temperatures between 300 and 990 K. *Int. J. Chem. Kinet*., **28**, 879-883.

Park, J. and Lin, M. C. (1997a). Laser-Initiated NO Reduction by NH_3: Total Rate Constant and Product Branching Ratio Measurements for the NH_2 + NO Reaction. *J. Phys. Chem*., **101A**, 5-13.

Park, J. and Lin, M. C. (1997b). A Mass Spectrometric Study of the NH_2 + NO_2 Reaction. *J. Phys. Chem*., **101A,** 14, 2643-2647.

Russell, J. J., Seetula, J. A. and D. Gutman (1988). Kinetics and Thermochemistry of CH_3, C_2H_5, and i-C_3H_7. Study of the Equilibrium R + HBr → R-H + Br. *J. A. C. S*., **110**, 3092-3096.

Silver, J. A. and Kolb, C. E. (1982). Kinetic Measurements for the Reaction of NH_2 + NO over the Temperature Range 294-1215 K. *J. Phys. Chem*., **86**, 3240-3246.

Vandooren, J., Bian, J. and van Tiggelen, P. J. (1994). Comparison of Experimental and Calculated Structures of an Ammonia-Nitric Oxide Flame. Importance of the NH_2 + NO Reaction. *Combust. Flame*, **98**, 402-410.

Wyatt, J. R., DeCorpo, J. J., McDowell, M. V. and Saalfeld, F. E. (1974). Simple Method for Adiabatically Sampling Reactive Gaseous Systems for Mass Spectrometry Analysis. *Rev. Sci. Instrum*., **45**, 916-919.

Wyatt, J. R., DeCorpo, J. J., McDowell, M. V. and Saalfeld, F. E. (1975). Sampling of Flow Systems at Atmospheric Pressure. *Int. J. Mass Spectrom. Ion Phys*., **16**, 33-38.

APPENDIX The Mechanism and Rate Constants[a] Used in the Kinetic Modeling of the NH_2 + NO_x System.

Reactions	A	*n*	E_a	Reactions	*A*	*n*	E_a
$NH_2+NO=NNH+OH$	8.40E+09	0.53	998 [b]	$NH+H=N+H_2$	3.00E+13	0	0
	9.19E+22	-3.02	9590 [c]	$NH+N=N_2+H$	3.00E+13	0	0
$NH_2+NO=N_2+H_2O$	8.28E+14	-0.93	-382 [b]	$NH+NH=N_2+2H$	2.50E+13	0	0
	3.40E+14	-0.98	-2604 [c]	$NH+NO=N_2+OH$	2.20E+13	-0.23	0
$NH_2+NO_2=H_2NO+NO$	6.56E+16	-1.44	268	$NH+NO=N_2O+H$	2.90E+14	-0.4	0
$NH_2+NO_2=N_2O+H_2O$	1.54E+16	-1.44	268	$NH+NO_2=N_2O+OH$	1.00E+13	0	0
$NH_3+OH=NH_2+H_2O$	2.00E+06	2.04	566	$NH+O=NO+H$	9.20E+13	0	0
$H_2NO+H=HNO+H_2$	3.00E+07	2	2000	$NH+OH=HNO+H$	2.00E+13	0	0
$H_2NO+H=NH_2+OH$	5.00E+13	0	0	$NH+OH=N+H_2O$	5.00E+11	0.5	2000
$H_2NO+M=H_2+NO+M$	7.83E+27	-4.29	60306	$NH_2+H=NH+H_2$	4.00E+13	0	3650
$H_2NO+M=HNO+H+M$	1.69E+32	-4.98	62312	$NH_2+HNO=NH_3+NO$	3.60E+07	1.6	-1252
$H_2NO+M=HNOH+M$	4.46E+30	-3.83	56888	$NH_2+NH=N_2H_2+H$	5.00E+13	0	0
$H_2NO+NH_2=HNO+NH_3$	3.00E+12	0	1000	$NH_2+NH_2=N_2H_2+H_2$	8.50E+11	0	0
$H_2NO+NO=HNO+HNO$	2.00E+07	2	13000	$NH_2+NH_2=NH_3+NH$	5.00E+13	0	10000
$H_2NO+NO_2=HONO+HNO$	6.00E+11	0	2000	$NH_2+O=HNO+H$	6.60E+14	-0.5	0
$H_2NO+O=HNO+OH$	3.00E+07	2	2000	$NH_2+O=NH+OH$	6.80E+12	0	0
$H_2NO+OH=HNO+H_2O$	2.00E+07	2	1000	$NH_2+OH+M=H_2NOH+M$	5.00E+17	0	0
$HNO+M=H+NO+M$	1.50E+16	0	48680	$NH_2+OH=NH+H_2O$	4.00E+06	2	1000
N_2/2.0/, H_2/2.0/, O_2/2.0/, H_2O/10.0/				$NH_3+H=NH_2+H_2$	6.40E+05	2.39	10171
$HNO+H=NO+H_2$	4.40E+11	0.72	650	$NH_3+M=NH_2+H+M$	2.20E+16	0	93470
$HNO+HNO=N_2O+H_2O$	4.00E+12	0	5000	$NH_3+NO_2=NH_2+HONO$	2.45E+11	0	25076
$HNO+NO=N_2O+OH$	2.00E+12	0	26000	$NH_3+O=NH_2+OH$	9.40E+06	1.94	6460
$HNO+NO_2=HONO+NO$	6.00E+11	0	2000	$NNH+H=N_2+H_2$	1.00E+14	0	0
$HNO+O=NO+OH$	1.00E+13	0	0	$NNH+NH_2=N_2+NH_3$	5.00E+13	0	0
$HNO+O_2=NO+HO_2$	1.00E+13	0	25000	$NNH+NO=N_2+HNO$	5.00E+13	0	0
$HNO+OH=NO+H_2O$	3.60E+13	0	0	$NNH+OH=N_2+H_2O$	5.00E+13	0	0
$HONO+H=HNO+OH$	5.64E+10	0.86	4969	$NNH=N_2+H$	1.00E+06	0	0
$HONO+H=NO+H_2O$	8.13E+06	1.89	3846	$NO+OH+M=HONO+M$	5.08E+23	-2.51	-68
$HONO+H=NO_2+H_2$	2.01E+08	1.55	6614	$NO_2+M=NO+O+M$	7.00E+19	0	53000
$HONO+HONO=NO+NO_2+H_2O$	9.69E+10	0	14132	N_2/1.7/, O_2/1.5/, H_2O/10.0/			
$HONO+NH=NH_2+NO_2$	1.00E+13	0	0	$NO_2+H=NO+OH$	8.40E+13	0	0
$HONO+O=NO_2+OH$	1.20E+13	0	6000	$NO_2+NO_2=NO+NO+O_2$	1.60E+12	0	26123
$HONO+OH=NO_2+H_2O$	4.00E+12	0	0	$NO_2+NO_2=NO_3+NO$	9.60E+09	0.73	20900
$N_2H_2+H=NNH+H_2$	5.00E+13	0	1000	$NO_2+O+M=NO_3+M$	1.30E+13	0	0
$N_2H_2+M=NNH+H+M$	5.00E+16	0	50000	$NO_2+O=NO+O_2$	3.90E+12	0	-238
$N_2H_2+NH=NNH+NH_2$	1.00E+13	0	1000	$NO_3+NO_2=NO+NO_2+O_2$	4.90E+10	0	2940
$N_2H_2+NH_2=NNH+NH_3$	1.00E+13	0	1000	$NO_3+OH=NO_2+HO_2$	1.00E+13	0	0
$N_2H_2+NO=N_2O+NH_2$	3.00E+12	0	0	$N_2O+M=N_2+O+M$	4.00E+14	0	56100
$N_2H_2+OH=NNH+H_2O$	1.00E+13	0	1000	N_2/1.5/, O_2/1.5/, H_2O/10.0/			
$N_2H_3+H=NH_2+NH_2$	1.60E+12	0	0	$O+H_2=H+OH$	5.00E+04	2.67	6300
$N_2H_3+OH=N_2H_2+H_2O$	1.00E+13	0	1000	$O+OH=H+O_2$	2.00E+14	-0.4	0
$N_2H_3+OH=NH_3+HNO$	1.00E+12	0	15000	$OH+H_2=H_2O+H$	2.10E+08	1.52	3540
$N_2H_4+OH=N_2H_3+H_2O$	4.00E+13	0	0	$OH+OH=H_2O+O$	4.30E+03	2.7	-2486
$N_2O+OH=N_2+HO_2$	2.00E+12	0	40000				

[a]Rate constants, defined by $k=AT^n \exp(-E_a/RT)$, are given in units of cm^3, mole and s; E_a is in units of cal/mole. [b]For 300-1000 K. [c]For 1000-2000K.